MOLECULAR AND CELLULAR BIOLOGY, Sept. 2008, p. 5348–5358 Vol. 28, No. 17
0270-7306/08/$08.00+0 doi:10.1128/MCB.02043-07

Nuclear Export Receptor Xpo1/Crm1 Is Physically and Functionally Linked to the Spindle Pole Body in Budding Yeast▽†

Anja Neuber,[1] Jacqueline Franke,[2] Angelika Wittstruck,[1] Gabriel Schlenstedt,[3] Thomas Sommer,[1] and Katrin Stade[1]*

Max Delbrück Centrum für Molekulare Medizin, Robert Rössle Strasse 10, 13092 Berlin, Germany[1]; Fachhochschule für Technik und Wirtschaft, Life Science Engineering, Blankenburger Pflasterweg 102, 13129 Berlin, Germany[2]; and Medizinische Biochemie und Molekularbiologie, Universität des Saarlandes, 66421 Homburg, Germany[3]

Received 13 November 2007/Returned for modification 28 December 2007/Accepted 16 June 2008

The spindle pole body (SPB) represents the microtubule organizing center in the budding yeast *Saccharomyces cerevisiae*. It is a highly structured organelle embedded in the nuclear membrane, which is required to anchor microtubules on both sides of the nuclear envelope. The protein Spc72, a component of the SPB, is located at the cytoplasmic face of this organelle and serves as a receptor for the γ-tubulin complex. In this paper we show that it is also a binding partner of the nuclear export receptor Xpo1/Crm1. Xpo1 binds its cargoes in a Ran-dependent fashion via a short leucine-rich nuclear export signal (NES). We show that binding of Spc72 to Xpo1 depends on Ran-GTP and a functional NES in Spc72. Mutations in this NES have severe consequences for mitotic spindle morphology in vivo. This is also the case for *xpo1* mutants, which show a reduction in cytoplasmic microtubules. In addition, we find a subpopulation of Xpo1 localized at the SPB. Based on these data, we propose a functional link between Xpo1 and the SPB and discuss a role for this exportin in spindle biogenesis in budding yeast.

In eukaryotes, the movement of proteins and RNAs between the nucleus and the cytoplasm is an essential cellular process that is mediated by soluble transport receptors (26, 52). In addition, the small GTPase Ran (Gsp1 in yeast) and its cytoplasmic and nuclear effectors are needed (12). Transport receptors involved in nuclear import reactions are usually termed importins, and they recognize their cargoes via a specific amino acid motif, the nuclear localization sequence, or NLS. By analogy, nuclear export reactions are mediated by so-called exportins. Xpo1 (also known as Crm1) was one of the first nuclear export receptors to be identified (23, 27, 50, 64) and recognizes a short leucine-rich amino acid sequence on its cargo, called a nuclear export signal, or NES. Numerous export cargoes have now been identified for the mammalian Crm1 protein, including protein kinase A inhibitor PKI, p53, and the human immunodeficiency virus protein Rev (20, 25, 66). In addition, Crm1 is involved in the nuclear export of several classes of RNAs such as viral pre-mRNAs, ribosomal RNAs, and snRNAs (54). In contrast, few NES-containing proteins have been identified in *Saccharomyces cerevisiae*. Although the budding yeast Crm1 orthologue Xpo1 is involved in nuclear export of Hog1 (19), Yap1 (76), Ssb1 (62), Ace2 (36), and Prp40 (46), few of the NESs involved have been characterized at a molecular level.

Recently, alongside its well-established role in nuclear export, mammalian Crm1 was shown to be involved in the control of centrosome duplication (71). Centrosomes function as microtubule (MT) organizing centers in mammalian somatic cells and direct the formation of a bipolar spindle during mitosis (reviewed in reference 6). In another study, Crm1 was found to bind to kinetochores, complex protein assemblies that are needed to establish the attachment of MTs to chromatin (4). These studies point to an unanticipated role of the exportin Crm1 in control of spindle assembly and cell cycle progression (8) and add another level of complexity to these processes since, so far, only certain importins and components of the Ran machinery are known to be involved in this process (11, 12, 28).

In budding yeast, the MT organizing center is known as the spindle pole body (SPB). Under the electron microscope, it is a multilayered high-molecular-weight structure embedded in the nuclear envelope (9). Cytoplasmic and nuclear surfaces of the SPB are known as outer and inner plaques and anchor both cytoplasmic and nuclear spindle fibers, which are spatially and functionally distinct (35). Nucleation of MTs at the SPB is mediated by the γ-tubulin (Tub4) complex that binds to the inner and outer plaques of the SPB via two specific Tub4 complex receptors, Spc110 and Spc72, respectively (56). Spc110 is located at the inner plaque of the SPB facing the nucleoplasm, and Spc72 binds at the cytoplasmic side of the SPB. Since budding yeast undergoes closed mitosis with no nuclear envelope breakdown, components of the nuclear spindle apparatus need to be imported into the nucleus from their site of synthesis in the cytoplasm. In addition, nuclear export might be required to clear the interior of the nucleus from spindle components after nuclear spindle disassembly. Curiously, information about this issue is scarce. For example, it has been shown that the γ-tubulin complex, which contains Spc97 and Spc98 as well as Tub4, is assembled in the cytoplasm and is subsequently imported into the nucleus via an NLS signal in Spc98 (53). However, given the fact that Tub4 complex is also needed at the cytoplasmic face of the SPB to

* Corresponding author. Mailing address: Max Delbrück Centrum für Molekulare Medizin, Robert Rössle Str. 10, 13092 Berlin, Germany. Phone: 49 30 9406 3736. Fax: 49 30 9406 3363. E-mail: kstade@mdc-berlin.de.

† Supplemental material for this article may be found at http://mcb.asm.org/.

▽ Published ahead of print on 23 June 2008.

nucleate cytoplasmic MTs, regulatory events must ensure the efficient and quantitative sorting of the Tub4 complex between the two compartments. How this is achieved and whether other components of the yeast SPB can act as import or export substrates is currently unknown.

In this study, we provide evidence that Spc72, a cytoplasmically localized protein of SPBs, interacts with the exportin Xpo1 in the yeast two-hybrid system and in in vitro binding experiments. Moreover, binding of Spc72 to Xpo1 is Ran dependent and mediated by an NES sequence in Spc72, which confers export activity to a reporter protein in vivo. Mutations of this NES in *SPC72* and *XPO1* alleles have severe consequences for spindle morphology, suggesting that in budding yeast the nuclear export machinery is involved in the biogenesis of the spindle apparatus.

MATERIALS AND METHODS

Microbial techniques and plasmids. Standard methods were used for the transformation and genetic manipulation of yeast (7). Rich medium (yeast extract, peptone, dextrose [YPD]) and synthetic minimal medium (synthetic dextrose [SD]) were prepared as described previously (60). Plasmids used in this study are listed in Table 1. Construction details are available on request.

Yeast strains, PCR-based gene tagging, and gene modification. PCR-based C-terminal green fluorescent protein (GFP) tagging of *XPO1* was done according to Longtine et al. (43) using either plasmid pFA6a-GFP-TRP1 (GSY835) or pFA6a-GFP-His3MX6 (tetrads from K842 background, resulting in KSY460 and KSY461, respectively) as a template. Yellow fluorescent protein (YFP) tagging of *XPO1* was done using plasmid pDH5 (Yeast Resource Center [YRC]) as a template and transforming the PCR product into CRY1 (*MAT***a** *ade2-1oc can1-100 his3-11,15 leu2-3,112 trp1-1 ura3-1*) (YRC), resulting in strain KSY592 [Xpo1-YFP (HIS3) *MAT***a** *ade2-1oc can1-100 his3-11,15 leu2-3,112 trp1-1 ura3-1*]. This strain was crossed to DHY45A [Spc29-cyan fluorescent protein (CFP) (KanMX) *MAT*α *ade2-loc ade3*Δ*100 can1-100 his3-11,15 leu2-3,112 ura3-1 TRP*] (YRC), resulting in the diploid KSY456. C-terminal tagging of Spc72 with GFP was done in a DF5 diploid using pFA6a-GFP-KanMX6 as a template, resulting in KSY581. Expression of GFP-fused Spc72 was confirmed under the microscope, and tetrads were dissected, resulting in strain KSY457 (Spc72-GFP). To obtain a GFP-tagged NES-mutated version of Spc72, DNA from KSY457 was isolated and used for a PCR containing a mutagenic forward primer resulting in KSY458 (Spc72*-GFP). For the construction of *XPO1* alleles with a GFP-tagged Spc72, KSY581 was transformed with a plasmid containing an *xpo1*::*LEU2* deletion construct (pKW435) (64). Correct integration at the *XPO1* locus was confirmed by PCR and Southern blotting. Subsequently, plasmids with *XPO1* (pKW440), *xpo1-1* (pKW457), and *xpo1-101* (pKS63) alleles were transformed into these cells, and after sporulation, tetrads were isolated, resulting in strains KSY582, KSY583, and KSY584, respectively. To obtain *SPC72* strains in which the NES was mutated, a PCR was set up using mutagenic primer sets and wild-type (WT) genomic DNA as a template. In a parallel reaction, the KanMX6 cassette was amplified from pFA6a-KanMX6. In a second PCR, products from the first PCRs were combined and amplified using a third set of primers. The resulting PCR product was gel purified, ethanol precipitated, and transformed into diploid yeast cells (DF5). Subsequently, cells were plated onto YPD-G418 plates (200 mg/liter geneticin). All PCR products obtained in this way were subcloned and subsequently sequenced to confirm the respective mutations. In all cases, strains were checked by PCR and Southern blotting for correct integration events. Strains testing positive on two successive rounds on YPD-G418 plates were used for targeted integration of pASF125 (67) and subsequent tetrad analysis, resulting in strains KSY462 (*SPC72* with GFP-Tub1) and KSY463 (*spc72** with GFP-Tub1). WT and *XPO1* strains with GFP-tagged tubulin were obtained by targeted integration of pASF125 in JD-4713c (65), *XPO1* (KWY120 [64]), *xpo1-1* (KWY121 [64]), and *xpo1-101* (KSY447), resulting in strains KSY318, KSY453, KSY454, and KSY455, respectively. For K842-derived WT and *spc72*Δ strains with GFP-Tub1, pASF125 was integrated into KSY361 (K842; *MAT***a**/α *SPC72*/*spc72*::*klTRP1*; *ade2-1 can1-100 leu2-3,112 his3-11,15 ura3 GAL* [*psi*$^+$] *ssd1-d2*) and tetrad analysis was done, resulting in KSY451 (*SPC72* with GFP-Tub1) and KSY452 (*spc72*Δ with GFP-Tub1). For the expression of Spc72-GFP versions under the *MET3* promoter, KSY361 was transformed with either pKS223 or pKS224. After sporulation, tetrads were dissected, and Ura$^+$ Trp$^+$ strains were isolated, resulting in KSY544 and KSY545, respectively.

TABLE 1. Plasmids

Name	Insert or description[a]	Source or reference
pACT-II	AD	37
pASF125	pRS306-GFP-Tub1	65
pGAD	AD	Clontech
pGBD	BD	Clontech
pDH5	YFP-HIS3	YRC
pFA series	GFP-KanMX cassette	41
pGEX-6P	GST	Amersham Biosciences
pGS978	YCp GAL-Gsp1	55
pGS979	YCp GAL-Gsp1^{G21V}	55
pGS980	YCp GAL-Gsp1^{T26N}	55
pGS488	GST-PKI-NES-GFP$_2$	42
pGS512	Xpo1-His$_6$	42
pGP63	AD-Spc72$^{1–271}$	37
pIA204-1	BD-Xpo1	P. Preker, UCSF[b]
pKS63	pRS313-xpo1-101	This study
pKS102	AD-Yap1$^{84–640}$	This study
pKS103	AD-Sgm1$^{218–707}$	This study
pKS104	AD-Spc72$^{3–433}$	This study
pKS105	AD-Hpa3	This study
pKS106	AD-Ltv1$^{55–463}$	This study
pKS107	AD-Sla2$^{309–720}$	This study
pKS108	AD-Nup49	This study
pKS109	AD-Nup42$^{1–379}$	This study
pKS186	GST-Spc72$^{3–433}$	This study
pKS187	GST-Spc72$^{3–433*}$	This study
pKS188	GST-Spc72$^{3–622}$	This study
pKS189	GST-Spc72$^{3–622*}$	This study
pKS192	AD-Spc72$^{3–433*}$	This study
pKS193	AD-Spc72	This study
pKS194	AD-Spc72*	This study
pKS195	NLS-Spc72-NES-GFP$_2$	This study
pKS197	GST-Spc72$^{3–96}$	This study
pKS198	GST-Spc72$^{3–129}$	This study
pKS199	GST-Spc72$^{3–163}$	This study
pKS202	GST-Spc72$^{3–398}$	This study
pKS223	MET3-Spc72-GFP	This study
pKS224	MET3-Spc72*-GFP	This study
pKS225	NLS-CtermSpc72-GFP$_2$	This study
pKS226	NLS-CtermSpc72*-GFP$_2$	This study
pKS227	MET3-NtermSpc72-GFP	This study
pKS228	MET3-NtermSpc72*-GFP	This study
pKW430	NLS-PKI-NES-GFP$_2$	62
pKW435	pBS-xpo1::LEU2	62
pKW440	pRS313-XPO1	62
pKW457	pRS313-xpo1-1	62
pKW581	His$_6$-Gsp1	42
pMK15	AD-Spc97	37
pMK151	AD-Spc110$^{1–204}$	37
pSG26	AD-Spc98	37
pSG46	AD-Tub4	37

[a] Mutations and the amino acid positions included in protein fragments are shown as superscripts. Plasmids containing two moieties of GFP are marked as GFP$_2$.
[b] UCSF, University of California, San Francisco.

Two-hybrid analyzes. Two-hybrid screening was performed as described previously (34). The bait plasmid pIA204-1 (pGBD-Xpo1, where pGBD is a GAL4 binding domain [BD] vector) was a gift of Pascal Preker (University of San Francisco, San Francisco, CA). pIA204-1 and a yeast genomic DNA library on pGAD (a GAL4 activation domain [AD] vector; Elizabeth Craig, University of Wisconsin, Madison, WI) were transformed separately into PJ69-4a (*MAT***a** *trp1-901 leu2-3,112 ura3-52 his3-200 gal4*Δ *gal80*Δ *LYS2*::*GAL1-HIS3 GAL2-ADE2 met2*::*GAL7 lacZ*), resulting in 3×10^6 transformants representing five copies of the yeast genome. After 10 days at 30°C on SD reporter plates lacking Trp, Leu, and His (SD-Trp$^-$-Leu$^-$-His$^-$), 264 colonies were isolated. Only 62 of these grew on SD-Trp$^-$-Leu$^-$-Ade$^-$ medium. Plasmids were rescued from these strains and retransformed into strain PJ69-4a containing plasmid pIA204-1.

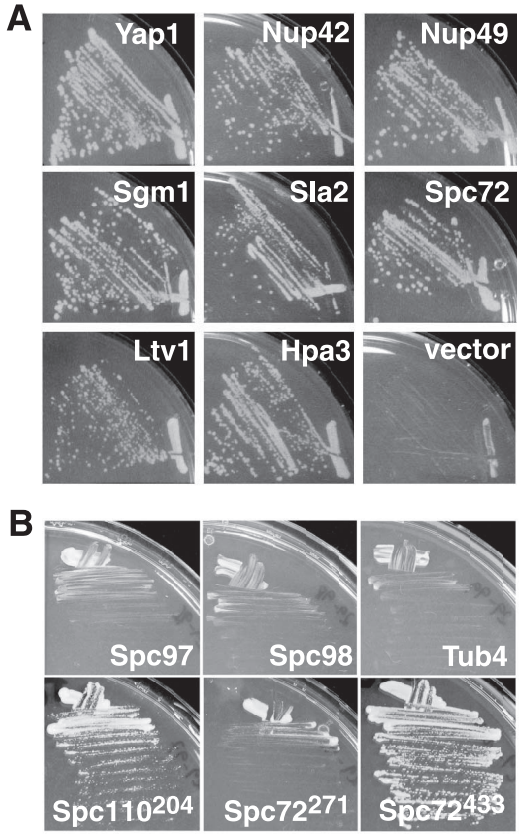

FIG. 1. Xpo1 interacts with the SPB proteins Spc72 and Spc110 by the yeast two-hybrid method. (A) Summary of the results obtained in the yeast two-hybrid screen. The following proteins or protein fragments were identified as Gal4-activation domain fusions in the screen: Yap (residues 184 to 640), Nup42 (1 to 379), Nup49, Sgm1 (218 to 707), Sla2 (309 to 720), Spc72 (3 to 433), Ltv1 (55 to 463), and Hpa3. No interaction can be detected between Gal4-AD and BD-Xpo1 in the empty vector control. For simplicity, gene names rather than protein fragment length were used. Interactions were tested on SD-Trp$^-$-Leu$^-$-His$^-$ plates. (B) Xpo1 interacts with the N terminus of Spc110 but not with components of the γ-tubulin complex. Gal4-AD fusions of full-length Spc97, Spc98, and Tub4 show no interaction when tested against BD-Xpo1. Gal4-AD-Spc110 comprises amino acids 1 to 204 from the N terminus of this protein (Spc110^{204}). For Gal4-AD fusions of Spc72, a 271-amino-acid (residues 1 to 271; Spc72^{271}) and a 430-amino-acid (residues 3 to 433; Spc72^{433}) fragment of the N terminus were tested. Interactions were tested on SD-Trp$^-$-Leu$^-$-His$^-$ plates.

Thirty-two plasmids that tested positive for interaction with pIA204-1 were subsequently sequenced. For the experiments shown in Fig. 1, interactions were tested on SD-Trp$^-$-Leu$^-$-His$^-$reporter plates. For the experiments in Fig. 4C, yeast cells were transformed with the plasmid combinations indicated in the figure. Plasmid-dependent growth was tested on SD-Trp$^-$-Leu$^-$ plates; interaction was checked on SD-Trp$^-$-Leu$^-$-His$^-$reporter medium.

In vitro binding assays. The purification of His_6-Gsp1 (yeast Ran) and Xpo1-His_6 from *Escherichia coli* was done as described previously (44). The loading of Gsp1 proteins with either GDP or GTP and subsequent purification has been described previously (5). Spc72 expression vectors were constructed as follows: the 430-amino-acid fragment of Spc72, residues 3 to 433 (Spc72^{433}) was subcloned from the pGAD vector into pGEX-6P-1 (Amersham Biosciences). To produce shorter versions of this protein, stop codons were introduced at the positions indicated in Fig. 4A by PCR mutagenesis using a QuikChange Kit (Stratagene). The same strategy was used to mutate the NES sequence at position 418 to 429 from LEKQINDLQIDK to LEKQINDAQADK. For expression of full-length Spc72, a PCR was set up using WT genomic DNA as a template. The resulting PCR product was used to replace Spc72^{433} in pGEX-6P-1. Mutation of the NES was achieved by site-directed mutagenesis. All glutathione (GSH) *S*-transferase (GST) fusion proteins were purified using GSH-Sepharose beads (Amersham Biosciences). Solution binding assays were done as described previously (44). WT and mutant PKI-NES peptides (64) used in competition assays were from Biosynthan.

Microscopy. Yeast cells with GFP-, YFP-, and CFP-tagged proteins were analyzed in vivo with an Axioplan II microscope equipped with an Axiocam digital camera and Axiovison III software (Zeiss) using appropriate filter setups. Processing of images was done using Adobe Photoshop, version 7. For CFP-YFP colocalization in the presence of Gsp1 mutants, strains were grown in synthetic minimal medium lacking uracil (SD-Ura$^-$) and containing galactose to select for the presence of plasmids and to induce protein expression. For each Gsp1 mutant, 100 random cells showing an Spc29-CFP signal were checked for the presence or absence of Xpo1-YFP at precisely the same spatial location in each cell. Results from three independent experiments were combined. To visualize nuclei, 1 μl of DAPI (4′,6′-diamidino-2-phenylindole; 1 mg/ml) was added to 1 ml of culture volume. To test the localization of GFP-Tub1 (KSY318) and Xpo1-GFP (KSY68) (64) in the presence or absence of nocodazole, strains were grown at 25°C to mid-log phase in SD-Ura$^-$ medium. Cultures were split in half, and either dimethyl sulfoxide alone or nocodazole in dimethyl sulfoxide was added to a final concentration of 30 μg/ml for 13 h according to the method of Amon (3). Expression of either WT or NES-mutated versions of Spc72-GFP under the control of the *MET3* promoter was achieved as follows. First, yeast cells (strains KSY544 and KSY545) were grown to mid-log phase in SD-Ura$^-$ medium supplemented with 1 mM methionine at 25°C to repress Spc72-GFP expression from plasmids pKS223 or pKS224, respectively. Subsequently, cells were washed into fresh medium lacking methionine for 1 h at 25°C to induce Spc72-GFP expression. Prolonged incubation under these conditions (more than 60 min) led to aggregate formation. Experiments with temperature shifts were done as described previously (64). For fluorescence intensity quantification of SPBs in strains KSY457 and KSY458, yeast were grown to mid-log phase at 25°C. For each strain, small budded cells with a GFP signal at the SPB were chosen, and a *z*-stack of nine sections at 0.2-μm intervals was captured for each individual cell. Only stacks covering the whole GFP signal (at least 30 stacks per strain) were included in the analysis. ImageJ software (1) was used to sum all nine sections of each stack. The integrated density around the SPB (circular region of interest; 21-pixel diameter) was recorded. For each cell, a corresponding background intensity was recorded and subtracted from the SPB intensity. The absolute values for the WT strains were set to 100 arbitrary units. For fluorescence intensity quantification of the SPB in yeast strains KSY582, KSY583, and KSY584, strains were grown to mid-log phase at 25°C, shifted to 37°C for 15 min, and analyzed within 10 min thereafter.

RESULTS

The SPB protein Spc72 is a novel interaction partner for Xpo1. In an effort to identify interaction partners for the exportin Xpo1, we performed a yeast two-hybrid screen using Xpo1 as a bait. In total, 32 plasmids were found to support growth on reporter medium in a bait-dependent fashion. These plasmids were sequenced and contained Gal4 activation domain in-frame fusions of the following open reading frames or fragments thereof: Nup42 (YDR192C; 11 plasmids), Yap1 (YML007W; 8 plasmids), Sgm1 (YJR134C; 4 plasmids), Spc72 (YAL047C; 2 plasmids), Hpa3 (YEL066W; 3 plasmids), Ltv1 (YKL143W; 2 plasmids), Sla2 (YNL243W; 1 plasmid) and Nup49 (YGL172W; 1 plasmid). A summary of the interactions found in the screen is shown in Fig. 1A. Three previously known Xpo1 interaction partners (Yap1, Nup42, and Nup49) were identified, demonstrating the usefulness of the two-hybrid method for this purpose. Yap1 contains a nuclear export sequence of the leucine-rich type and acts as an export substrate for Xpo1 (76) whereas Nup42 and Nup49 (48) are structural components of the nuclear pore complex (NPC) through which all nucleocytoplasmic trafficking occurs (18, 69). Sgm1, Sla2, Spc72, Ltv1, and Hpa3 represent novel interaction partners for Xpo1. These proteins are involved in a variety of cellular pro-

cesses such as membrane cytoskeleton assembly (Sla2 [32]), mitotic spindle assembly (Spc72 [35]), and chromatin modification (Hpa3 [77]). For Ltv1, a role in the Xpo1-mediated export of small ribosomal subunits has recently been shown (59). No function has been assigned to Sgm1 so far, and with the exception of Ltv1, none of the proteins found in our screen has been analyzed with respect to a possible function in nuclear export. Although Sgm1 and Spc72 have been identified in other two-hybrid screens as Xpo1 interactors, they were not analyzed further (33, 36).

In higher eukaryotes, the Ran-GTPase system and certain transport receptors, apart from their well-established function in nuclear transport processes, were recently shown to be involved in mitotic spindle assembly (10, 47, 73, 74). Spc72 was particularly interesting since it is a cytoplasmic protein that functions as a structural component of the yeast SPB. This supramolecular protein complex is embedded in the nuclear membrane and is required to nucleate cytoplasmic and nuclear MTs for mitotic spindle assembly (35). During cytoplasmic MT nucleation, Spc72 interacts with the γ-tubulin complex consisting of Spc97, Spc98, and Tub4 (39). We wanted to test whether these proteins would also interact with Xpo1 in the yeast two-hybrid system. To this end, we performed a directed two-hybrid analysis with plasmids obtained from the Knob and Schiebel laboratory (39). Figure 1B shows the result of this experiment: the three subunits of the γ-tubulin complex, Spc97, Spc98, and Tub4, do not interact with Xpo1. However, we find that the N terminus of Spc110 (amino acids 1 to 204), another protein of the SPB, does indeed interact with Xpo1. Interestingly, a shorter version of the N terminus of Spc72 (amino acids 1 to 271 [Spc72^{271}]) fails to interact with Xpo1. Thus, in the two-hybrid assay Xpo1 interacts with at least two components of the yeast SPB, Spc72 and Spc110, which are required to nucleate MTs of the mitotic spindle.

Xpo1 is localized at the SPB in vivo. In higher eukaryotic cells, the receptor for leucine-rich NESs, Crm1, localizes to the nuclear interior and at NPCs, in line with its proposed function as an exportin mediating nuclear export of substrate proteins (24). More recently, Crm1 was shown to bind to kinetochores as well as centrosomes, two high-molecular-weight protein complexes which in concert with chromatin organize assembly of the mitotic spindle (4, 22). Since Xpo1 is the yeast orthologue of Crm1 and since the SPB is the functional equivalent of centrosomes in yeast, we wanted to know whether the two-hybrid data obtained for Spc72 and Spc110 would hint at a role of Xpo1 in the SPB, apart from its well-established function in nuclear export. In an effort to address this issue, we genomically tagged *XPO1* with GFP and localized the fusion protein in living yeast. The upper panels in Fig. 2A show that Xpo1-GFP, in addition to its expected presence in the nucleus and at the nuclear envelope, can be detected at distinct foci at the nuclear periphery, identical to the localization pattern of SPBs. The same localization pattern is observed for a mutant allele of *XPO1* (Xpo1-1–GFP). We also tested whether Xpo1 localization is MT dependent. To this end, experiments were performed in the presence and absence of nocodazole, an MT-depolymerizing drug. Even after prolonged incubation with nocodazole, Xpo1-GFP signals are detected in SPB-like dots, indicating that its localization pattern is not MT dependent (see Fig. S2 in the supplemental material). Additionally, we

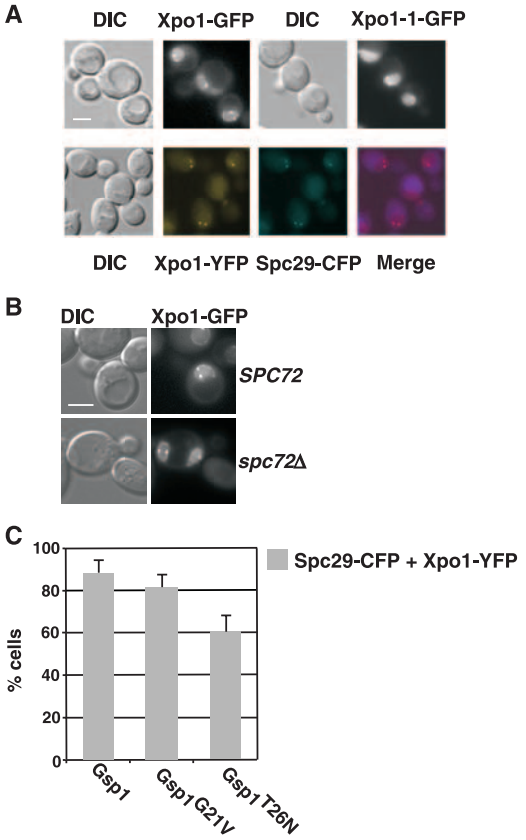

FIG. 2. Some fraction of Xpo1 localizes at the SPB in vivo. (A) Xpo1-GFP (strain GSY835) and Xpo1-1-GFP (KSY69 [64]) localize at distinct dots at the nuclear periphery (top). Xpo1-YFP and Spc29-CFP colocalize (Merge) at the SPB (KSY456) (bottom). Bar, 5 μm. (B) Xpo1-GFP is not lost from the SPB in an *spc72*Δ strain. Shown is a comparison of Xpo1-GFP localization in *SPC72* (KSY460) and an *spc72*Δ mutant (KSY461). In the *spc72*Δ strain, two nuclei are present in one cell, indicative of a defect in nuclear migration (31). Bar, 5 μm. (C) Perturbations in nuclear Gsp1-GTP concentration influence binding of Xpo1-YFP at the SPB. Plasmid-borne WT (Gsp1) and mutant forms of Gsp1 locked in either the GTP-bound (Gsp1-G21V) or nucleotide-free (Gsp1-T26N) state, respectively, were overexpressed from the *GAL* promoter in KSY456. A total of 100 random cells showing an Spc29-CFP signal were inspected for the presence or absence of Xpo1-YFP at the SPB, as described in the Materials and Methods section. Error bars (standard deviations) are shown. DIC, differential interference contrast optics.

performed a double labeling experiment, depicted in the lower row of Fig. 2A, using chromosomally tagged Xpo1-YFP and Spc29-CFP, a protein of the central plaque of the SPB (16). In this experiment, the two fluorescence signals overlap (Fig. 2A, Merge), suggesting the presence of some Xpo1 at SPBs. To test if Spc72 was the binding partner of Xpo1 at SPBs, a yeast strain with a deletion of *SPC72* (*spc72*Δ) was GFP tagged at the *XPO1* locus. As can be seen in Fig. 2B, lower panel, Spc72 is not required for Xpo1 binding at SPBs since the Xpo1-GFP signal is still detected at distinct dots at the nuclear rim in *spc72*Δ cells. This suggests that Xpo1 might have other binding partners at the SPB.

At the NPC, some nuclear transport receptors interact with nucleoporins via a specific motif found in these nucleoporins, the FG repeat (18). For SPB proteins, FG repeats have not

been reported, and it is therefore tempting to speculate that Xpo1 targeting to SPBs is mediated by an NES in one or more of the SPB proteins. Thus, it can be predicted that Xpo1 should bind to SPBs only in the presence of Gsp1-GTP since Xpo1 binds its NES-containing cargoes in a cooperative fashion with Gsp1-GTP (40, 44). To test this hypothesis, we analyzed the colocalization of Xpo1-YFP with Spc29-CFP in the presence of WT Gsp1 and two Gsp1 mutants, Gsp1-G21V and Gsp1-T26N, overexpressed from plasmids in vivo (57). All these versions of Gsp1 accumulate in the nucleus of WT cells; each, however, has a different GTP status. Whereas Gsp1 can bind and hydrolyze GTP normally, Gsp1-G21V is locked in the GTP-bound state. Gsp1-T26N, on the other hand, has a very low affinity for nucleotides and inhibits the Ran cycle via its tight interaction with the RanGEF Rcc1/Prp20 (14). Cells in which Gsp1-G21V is overexpressed from the *GAL* promoter are viable but show a cytoplasmic mislocalization of nuclear proteins. In addition, these cells have an export defect for poly(A)$^+$ RNA, indicative of an inability to hydrolyze GTP by Gsp1-G21V, which is required for normal nuclear transport (57). In contrast, cells with a WT version of Gsp1 show a normal distribution of poly(A)$^+$ RNA and nuclear proteins, suggesting that overproduction of Gsp1 is not toxic per se. As is shown in Fig. 2C, 87% (± 5%) of the cells colocalize Xpo1-YFP with Spc29-CFP in the presence of overexpressed WT Gsp1 whereas some Xpo1-YFP signal is lost from the dot at the nuclear rim in the presence of GTP-locked Gsp1-G21V mutant (81% ± 4.8% cells with both proteins colocalizing). However, only 60% (± 6.7%) of the cells show Xpo1-YFP/Spc29-CFP colocalization in the presence of Gsp1-T26N, indicating that binding of Xpo1-GFP at the SPB is indeed dependent on the GTP status of the cell.

Taken together, our in vivo localization data demonstrate that a subpopulation of Xpo1 is localized at SPBs. Since Xpo1-GFP is not lost from SPBs in an *spc72*Δ mutant, binding must be dependent on one or more of the other SPB components. This binding could be NES dependent since SPB localization of Xpo1 occurs in a Gsp1-GTP-dependent fashion.

Xpo1 binds to a subfragment of Spc72 in a Gsp1-GTP- and NES-dependent manner in vitro. In combination, the two-hybrid data and the in vivo localization data suggested that a subpopulation of Xpo1 is localized at the SPB and that Spc72 might be one of several interaction partners at this organelle. Since Xpo1 localization is modulated by Gsp1, its SPB association could be dependent on an NES-containing SPB protein. By visual inspection, the Spc72^{433} sequence contains several amino acid stretches which resemble leucine-rich NESs. We therefore wanted to test the possibility thatSpc72^{433} might bind to Xpo1 via one or more of these putative NESs. In the cell, the binding of Ran-GTP and an NES-containing protein to Xpo1 is highly cooperative, and accessory factors support complex formation (17, 42, 49, 68). However, most NESs are rather weak, and the isolation of trimeric complexes from cellular extracts has been technically challenging (40, 41, 44). To circumvent these problems, we expressed the fragment of Spc72 identified in the two-hybrid screen in bacteria and performed in vitro binding assays in the presence of recombinant Gsp1 and Xpo1. In this type of experiment, Xpo1 binds to its substrates in a Gsp1-GTP- and NES-dependent fashion without the addition of accessory proteins. Moreover, this binding can be competed by an excess of NES peptide but not mutated versions thereof (44). The left panel in Fig. 3A shows a control experiment in which a fusion protein between GST and the NES sequence from PKI was bound to GSH beads. Only in the presence of Gsp1-GTP can recombinant Xpo1 bind to the GST-NES beads (lane 5), whereas no binding is observed in the absence of Gsp1 (lane 1) or in the presence of Gsp1-GDP (Fig. 3A, lane 3). In the experiment shown in the right panel of Fig. 3A, an N-terminal fragment of Spc72 (Spc72^{433}) was expressed as a GST fusion and bound to GSH-Sepharose beads. In the presence of Gsp1-GTP, recombinant Xpo1 can bind to the GST-Spc72^{433} beads (lane 9), whereas no binding is observed in the Gsp1-GDP control lane (lane 7). To test whether excess amounts of NES peptide can compete binding of Xpo1 to GST-Spc72^{433}, we next included a synthetic PKI-NES peptide in the binding reaction. As can be seen in Fig. 3B, binding of Xpo1 to GST-Spc72^{433} is reduced when additional NES peptide is present (compare lanes 1 and 3). However, this binding is not reduced when a mutated, nonfunctional version of the PKI-NES peptide (64) is present in the reaction (lanes 5 and 6). From these experiments we conclude that Xpo1 binds to Spc72^{433} in a Gsp1-GTP- and NES-dependent fashion, which indicates that these proteins can form a typical export complex.

Spc72 contains an NES. The in vitro experiments shown in Fig. 3A and B suggested that Spc72 could act as an export substrate for Xpo1. A prerequisite for such an interaction is a leucine-rich NES. Figure 4A shows a schematic drawing of the complete Spc72 sequence with mapped binding sites for known interaction partners (29, 39, 70) and 12 short leucine-rich amino acid stretches which potentially could serve as NESs. To identify one or more NES(s) in Spc72^{433}, we expressed the fragments of the protein depicted in Fig. 4A and tested for binding to Xpo1 in the in vitro binding assay. Figure 4B summarizes the results of these experiments: only the longest fragment of Spc72 comprising amino acids 3 to 433 (Spc72^{433}) can bind to Xpo1 in the presence of Gsp1-GTP (lane 7). All shorter versions fail to bind to Xpo1 in the presence of Gsp1-GTP (Fig. 4B, lanes 3 to 6; compare with the GST-NES control in lane 1 and GST-only control in lane 2), indicating that it is the most-C-terminal NES-like sequence between amino acids 418 to 429 in Spc72^{433} that is needed for binding to Xpo1. LEKQINDLQIDK$_{418–429}$ conforms to the NES consensus deduced from a variety of NES-containing proteins (30, 41).

If a stretch of amino acids is predicted to function as an NES, it should lose this function when mutated at key residues of the consensus (30). We therefore introduced leucine/isoleucine-to-alanine mutations at positions 425 and 427, resulting in LEKQINDAQADK$_{418–429}$ and tested binding of this NES-mutated Spc72^{433} (Spc^{433}*) to Xpo1 in the presence of Gsp1-GTP. As is shown in Fig. 4B, lane 8, binding to Xpo1 is lost when Spc72^{433} is mutated at positions 425 and 427, indicating that this sequence between residues 418 and 429 can indeed function as an NES recognized by Xpo1. We also expressed full-length WT and NES-mutated Spc72 in bacteria although this was technically difficult due to the tendency of Spc72 to form aggregates. In binding experiments, these proteins gave inconsistent binding patterns (data not shown). To circumvent the problems with recombinant full-length Spc72, we performed a directed yeast two-hybrid analysis to test for an in-

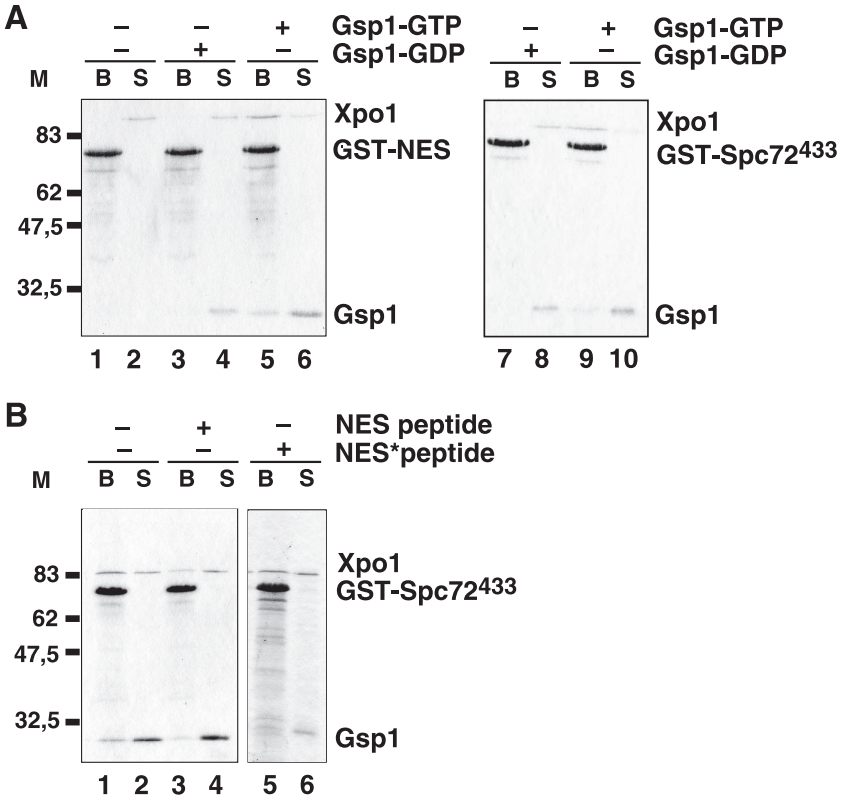

FIG. 3. Xpo1 binds a fragment of Spc72 in a Gsp1- and NES-dependent manner in vitro. (A) GST-NES as a control or GST-Spc72^{433} (GST fused to amino acids 3 to 433 of Spc72) (18 μg per reaction) was immobilized on GSH-Sepharose and incubated for 30 min at 4°C with 15 μg of recombinant Gsp1-GDP and Gsp1-GTP and 12 μg of Xpo1 as indicated. After binding, the supernatant (S) was precipitated with trichloroacetic acid and resuspended in sodium dodecyl sulfate sample buffer. Bound material was washed three times and subsequently eluted from the beads (B) with sodium dodecyl sulfate sample buffer. All samples were analyzed by sodium dodecyl sulfate-polyacrylamide gel electrophoresis and Coomassie blue staining. (B) As in panel A, GST-Spc72^{433} was immobilized on GSH beads and incubated with Gsp1-GTP and Xpo1. In addition, synthetic peptides comprising either the WT PKI-NES (89 μg) or a mutated version thereof (NES*; 85 μg) were included in the binding reaction. Samples were further processed as described in panel A. M, molecular mass (in kilodaltons).

teraction with Xpo1. As can be seen in Fig. 4C, Xpo1 interacts only with full-length Spc72 with a WT NES (Fig. 4C, upper row, pGBD-Xpo1/pGAD-Spc72) but not when this sequence is mutated (Fig. 4C, upper row, pGBD-Xpo1/pGAD-Spc72*), indicating that the NES at position 418 to 429 (NES$_{418–429}$) is the only functional NES in Spc72. Shorter constructs with Spc72^{433} and Spc72^{433}* were also included in the analysis. Positive Xpo1/Spc72^{433} interaction (pGBD-Xpo1/pGAD-Spc72^{433}) is lost when the NES is mutated (pGBD-Xpo1/pGAD-Spc72^{433}*), confirming the results obtained in the in vitro binding assays (Fig. 4B). No interaction is seen with the empty vector control (pGBD/pGADSpc72^{433}). Taken together, our results indicate that amino acids LEKQINDLQI DK$_{418–429}$ in Spc72 can function as an NES in vitro and in vivo.

NES$_{418–429}$ has nuclear export activity in vivo. To test whether LEKQINDLQIDK$_{418–429}$ had any export function in vivo, we used a GFP reporter assay (64). In this assay, a tandem GFP is fused to an NLS and an NES derived from the protein of interest, for example, PKI (72). In WT cells, this fusion protein shuttles between the nucleus and the cytoplasm and hence can be localized to both compartments. However, when this protein is expressed in *xpo1* mutants in which nuclear export is substantially slowed down compared to WT cells, the protein accumulates in the nucleus (64). Figure 5A shows a comparison of *XPO1* and *xpo1-1* cells expressing two versions of the GFP reporter protein at 37°C. As can be seen in the upper row of Fig. 5A, the NLS-PKI-NES-GFP reporter is detected in the cytoplasm and nucleus of WT cells even at 37°C. The reporter construct in which the PKI-NES was replaced by Spc72 LEKQINDLQIDK$_{418–429}$ also localizes to the nucleus and cytoplasm when expressed in *XPO1* cells (Fig. 5A, upper row, right panels). However, both GFP reporter proteins accumulate in the nucleus of the *xpo1-1* strain when cells are incubated at the nonpermissive temperature (Fig. 5A, lower row). This indicates that LEKQINDLQIDK$_{418–429}$ has an export activity in vivo.

We also wanted to test NES$_{418–429}$ in its native protein context. However, the amount of Spc72-GFP when expressed from its endogenous promoter was rather low (Fig. 6), making it impossible to detect any non-SPB-bound Spc72-GFP which might have accumulated in the nucleus, as would be expected for *xpo1* mutants. On the other hand, use of regulatable promoters such as *GAL1-10* and *MET3* leads to formation of aggregates when Spc72-GFP is overexpressed (63; see also Fig. S5 in the supplemental material). We therefore expressed the C- and N-terminal halves of Spc72 individually as GFP fusions.

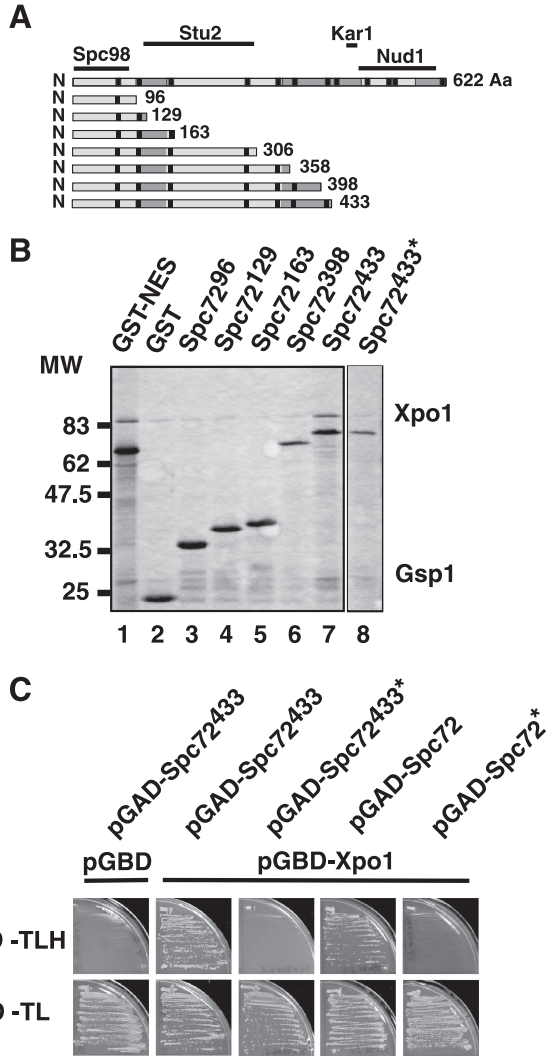

FIG. 4. $Spc72^{433}$ contains a leucine-rich NES-like amino acid motif at position 418 to 429 that mediates binding to Xpo1 in vitro and in vivo. (A) Schematic drawing of the full-length Spc72 sequence with known binding partners (black bars) and 12 putative NES-like motifs (black squares) indicated. Regions shown in dark gray indicate putative coiled-coil motifs. Spc72 fragments of indicated lengths were expressed as GST fusions in *E. coli* and used in the binding assays summarized in panel B. (B) Binding assay with Spc72 fragments. Binding assays were done exactly as described in the legend of Fig. 3A, and only binding to the beads is shown. GST fusions of Spc72 fragments of indicated lengths (lanes 3 to 8; 18 μg each) were bound to GSH beads and incubated with Gsp1-GTP (15 μg) and Xpo1 (12 μg). Lane 8 contains an NES-mutated version of GST-$Spc72^{433}$ ($Spc72^{433}$*). As positive and negative controls for binding, GST-PKI-NES (18 μg; lane 1) and GST alone (18 μg; lane 2) are shown. (C) Yeast two-hybrid analysis of Spc72 fragments and full-length proteins. PJ69-4a cells were transformed with either pGBD or pGBD-Xpo1, respectively, and a WT (pGAD-$Spc72^{433}$) or NES-mutated (pGAD-$Spc72^{433}$*) version of $Spc72^{433}$. pGAD-Spc72 and NES-mutated pGAD-Spc72* were also tested. Interactions were tested on SD-Trp^--Leu^--His^- medium (SD −TLH). Plasmid-dependent growth was controlled on SD-Trp^--Leu^- medium (SD −TL).

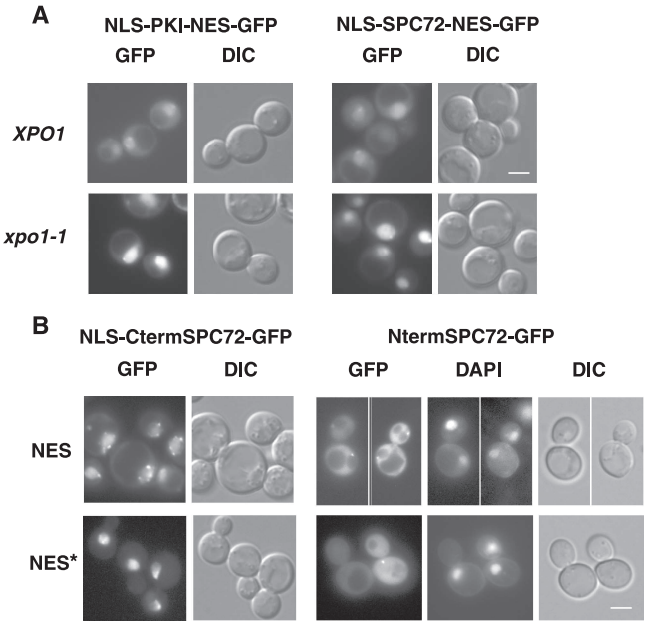

FIG. 5. The leucine-rich NES-like sequence at position 418 to 429 of Spc72 mediates nuclear export in vivo. (A) Summary of the results obtained from a nuclear export reporter assay in vivo. The NES sequence from PKI (NLS-PKI-NES-GFP; pKW430) and the putative Spc72 NES $LEKQINDLQIDK_{418–429}$ (NLS-SPC72-NES-GFP; pKS195) were expressed as GFP fusions in living yeast. In *XPO1* cells (KWY120), due to the NES and NLS, the proteins shuttle between the nucleus and cytoplasm at 37°C and can be localized to both compartments (GFP, upper row). However, in the *xpo1-1* temperature-sensitive mutant (KWY121), export activity is slowed down substantially at 37°C (GFP, lower panels), and therefore even in the presence of an intact NES, the reporter proteins accumulate in the nucleus. Bar, 5 μm. (B) Localization of GFP-tagged N and C termini of Spc72. The N-terminal 433 amino acids of Spc72 (NtermSPC72-GFP) were fused to GFP in either their WT (NES; pKS227) or NES-mutated (NES*; pKS228) version. The Spc72 C terminus comprising amino acids 396 to 622 (NLS-CtermSPC72-GFP) was fused to two moieties of GFP either in its WT (NES; pKS225) or NES-mutated (NES*; pKS226) version. In addition, the C-terminal fusion proteins contain an artificial NLS sequence to allow for nuclear accumulation. All fusion proteins were expressed in cells WT for *XPO1* and *SPC72* (KSY57) at 25°C. Bar, 5 μm. DIC, differential interference contrast optics.

All fusion proteins are larger than 70 kDa in size to prevent passive diffusion through the NPC. First, we expressed the C terminus of Spc72 (amino acids 396 to 622 [NLS-CtermSPC72-GFP]) in its WT (NES) and NES-mutated version (NES*) as NLS-GFP fusion proteins (Fig. 5B). An artificial NLS was included to allow for shuttling of the proteins between the nuclear and cytoplasmic compartments. Whereas the WT C terminus (NES) is localized to the nucleus, cytoplasm, and nuclear periphery in WT cells, its NES-mutated version (NES*) is completely targeted to the nucleus due to the artificial NLS sequence. This indicates that $NES_{418–429}$ can function as an NES within the C-terminal half of Spc72. In a similar experiment, we fused the N terminus of Spc72 (amino acids 1 to 433 [NtermSPC72-GFP]) including either a WT (NES) or a mutated $NES_{418–429}$ (NES*) to GFP. In this construct, no artificial NLS is present. As can be seen in Fig. 5B (right panel, upper row), Nterm-SPC72-GFP localizes to the cytoplasm of WT cells, with some GFP dots at the nuclear periphery which could be SPBs. The nucleus is completely devoid of any GFP signal (nuclear exclusion) (Fig. 5B, right, compare DAPI and GFP panels). However, when $NES_{418–429}$ is mutated, a significant proportion of NtermSPC72-GFP (NES*) becomes nu-

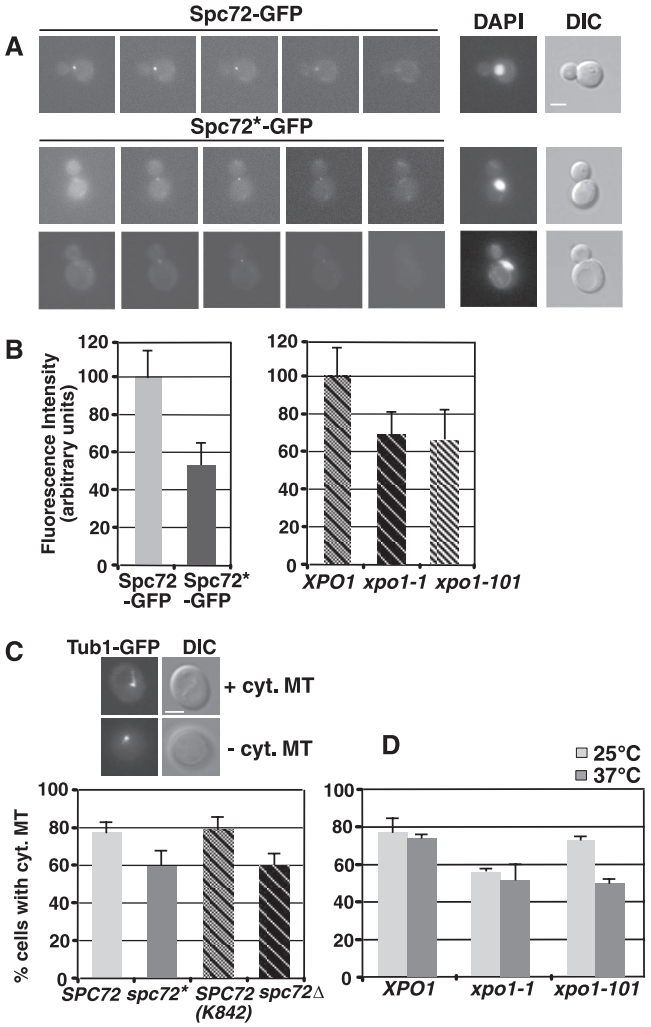

FIG. 6. Mutations in the NES sequence of Spc72 influence its binding to the SPB and affect spindle morphology in vivo. (A) Localization of WT (Spc72-GFP) and NES-mutated Spc72-GFP (Spc72*-GFP) in vivo. The upper row shows *z*-axis plane fluorescence images of a WT yeast cell in which *SPC72* is genomically tagged with GFP (KSY457). The two lower rows show individual cells of a strain (KSY458) in which the $NES_{418–429}$ of Spc72-GFP has been mutated as described in Materials and Methods. Exposure time was the same for all samples. For comparison, the position of the cell nucleus is indicated by DAPI staining. Bar, 5 μm. (B) Fluorescence intensity quantification of Spc72-GFP at the SPB. Haploid strains of *SPC72* and *XPO1* alleles were grown to mid-log phase and processed for fluorescence intensity quantification as described in Materials and Methods. The left panel compares the GFP fluorescence intensity at the SPB of a WT (Spc72-GFP; strain KSY457) and an NES-mutated (Spc72*-GFP; strain KSY458) version of Spc72-GFP. The right panel shows a similar experiment in which Spc72-GFP fluorescence was measured at SPBs of three different *XPO1* alleles: WT (KSY582), *xpo1-1* (KSY583), and *xpo1-101* (KSY584). The mean intensity ± standard deviation of at least 30 SPBs is shown for each strain. (C) The formation of cytoplasmic MT (cyt. MT) is impaired in an *spc72** mutant in vivo. For *SPC72* WT (KSY462), *spc72** mutant (spc72*; KSY463), another WT (KSY451), and *spc72*Δ strains (KSY452), a GFP-tagged copy of *TUB1* was integrated at the *URA* locus. In each experiment, 200 cells in the G_1 phase of the cell cycle (see example cells) were visually inspected for the presence or absence of cytoplasmic MTs as described previously (58). Error bars (standard deviations) are shown. Size bar, 5 μm. (D) Formation of cytoplasmic MTs is reduced in *XPO1* alleles in vivo. GFP tagging of *TUB1* in *XPO1* (KSY453), *xpo1-1* (KSY454), and *xpo1-101* (KSY455); temperature shifts; and cell classification were done as described in Materials and Methods. DIC, differential interference contrast optics.

clear (Fig. 5B; DAPI and GFP signals overlap). Since in this case no artificial NLS was included in the fusion protein, this indicates that the N-terminal part of Spc72 can be imported into the nucleus. Whether this nuclear localization is mediated by an endogenous NLS in Spc72 or whether the protein is imported via an adaptor (piggyback mechanism) is unknown at present. But in any case, our data indicate that Spc72 has a functional $NES_{418–429}$ in vivo.

Mutations in *SPC72* and *XPO1* result in a defect in cytoplasmic MT formation in vivo. To test whether $NES_{418–429}$ had any impact on the functions of Spc72 in vivo, we generated yeast strains carrying either a WT (Spc72-GFP) or an NES-mutated GFP-tagged version of Spc72 (Spc72*-GFP) under the control of its own promoter. Under normal laboratory conditions, no difference in growth could be observed. Figure 6A shows that WT Spc72-GFP localizes at a distinct dot at the nuclear periphery, in accordance with its proposed function as an SPB protein (upper row). In a strain carrying a mutated $NES_{418–429}$ (Fig. 6A, Spc72*-GFP), a strongly reduced GFP signal was visible at the nuclear periphery with a faint increase of GFP fluorescence in the cytoplasm, suggesting that despite its mutated $NES_{418–429}$, Spc72*-GFP might still be localized to the cytoplasm but might no longer be able to associate efficiently with SPBs. We used fluorescence intensity quantification to test this possibility. The left panel in Fig. 6B shows the result of this analysis: for Spc72*-GFP, the fluorescence intensity (in arbitrary units) is only half (52.8 ± 12.5) of what can be observed for WT Spc72-GFP (100 ± 15.3), indicating a loss of fluorescence from the SPB. A similar experiment was performed with a WT and two conditional *xpo1* alleles. In these strains, Spc72-GFP also localizes to the SPB (data not shown). To exclude the possibility of an allele-specific defect of *xpo1-1*, we included the *xpo1-101* allele in the analysis. This novel *xpo1* allele has a defect in nuclear export but carries a different mutation than *xpo1-1* (A. Neuber and K. Stade, unpublished data). The right panel in Fig. 6B shows that, compared to a WT *XPO1* strain (100 ± 15.9), Spc72-GFP fluorescence is significantly reduced in *xpo1-1* (68.5 ± 13.0) and *xpo1-101* cells (67.7 ± 15.0), respectively. By immunoblot analysis, the amounts of Spc72-GFP and Spc72*-GFP were comparable, indicating that the loss of GFP fluorescence from the nuclear periphery did not result in degradation of the protein (data not shown). We therefore reasoned that if the amount of NES-mutated Spc72 is reduced at SPBs, the nucleation of cytoplasmic MTs and, hence, mitotic spindle formation should be impaired, as is the case in an *spc72* deletion strain (31, 63). To address this question, we integrated a GFP-tagged copy of *TUB1* at the *URA* locus in *SPC72* and *spc72** strains and analyzed the extent to which cytoplasmic MTs could be formed on SPBs. In the G_1 phase of the cell cycle, the SPB usually appears as a single dot with MTs emanating from it into the cytoplasm (58, 75). Between 150 and 200 cells in the G_1 phase were selected and inspected for the presence or absence of MT asters (Fig. 6C, GFP-Tub1, top panel). As a control, we included an *spc72* deletion strain in our analysis which is known to lack a substantial amount of cytoplasmic MTs (31, 63). As can be seen in Fig. 6C, formation of cytoplasmic MTs can be observed in only 60.7% (± 7.1%) of the cells carrying an NES mutation (*spc72**) compared to WT cells with 76.3% (± 6.5%). The WT strain derived from the K842 background (*SPC72* (K842);

78.6% ± 7.0%) and the corresponding *spc72* deletion strain (*spc72*Δ; 60.4% ± 6.5%) show similar results, indicating that the mutation of $NES_{418–429}$ might indeed perturb function of Spc72 at the SPB.

In a similar experiment, we used *xpo1* alleles for our analysis. If Spc72 is an export substrate for Xpo1, nuclear accumulation of Spc72 in *xpo1* mutants should lead to a shortage of the protein in the cytosol and, hence, to a defect in formation of cytoplasmic MTs. As can be seen in Fig. 6D, the different *xpo1* alleles indeed have similar phenotypes: at the permissive temperature, 77.1% (± 6.6%) of WT cells (*XPO1*) form cytoplasmic MTs at the SPB whereas in the *xpo1-1* strain (56.0% ± 0.7%) and the *xpo1-101* allele (73.8% ± 1.4%), this number is reduced. At 37°C, this phenotype is more pronounced: only 52.7% (± 7.7%) of *xpo1-1* cells have cytoplasmic MTs left, and in the *xpo1-101* allele, 47.2% (± 1.8%) of the cells are still equipped with cytoplasmic MTs. Taken together, our in vivo data suggest that the mutation of $NES_{418–429}$ of Spc72 leads to loss of the protein from SPBs and subsequently to a reduction of MTs on the cytoplasmic side of the nuclear envelope. In addition, mutations in the nuclear export receptor Xpo1 result in a similar phenotype with respect to cytoplasmic MT morphology.

DISCUSSION

In higher eukaryotic cells, evidence is accumulating that components of the nuclear transport machinery are involved in nuclear functions apart from nucleocytoplasmic trafficking. In metazoans, nuclear envelope formation, NPC assembly, and formation of the mitotic spindle have been shown to be dependent on certain nuclear transport receptors and the Ran-GTPase system (12, 45). In fission and budding yeast, the Ran system was identified as a regulator for the MT cytoskeleton and NPC assembly (21, 38, 51, 55). Since the Ran machinery, transport receptors, and NPC proteins are highly conserved, it is reasonable to assume that in budding yeast the nuclear transport apparatus is engaged in other nuclear functions as well. However, experimental evidence is scarce, and since budding yeast cells do not dissolve their nuclear envelopes during mitosis, it has been argued that spindle assembly must be functionally distinct from the analogous process in higher eukaryotes (13).

In this study, we provide evidence that nuclear protein export and spindle morphogenesis may be linked in budding yeast. In an effort to identify novel export substrates for the exportin Xpo1, we performed a yeast two-hybrid screen. Among known interactors of Xpo1 such as Yap1, Nup42, and Nup49 (48, 76), we identified a group of proteins that previously had not been studied in the context of nuclear transport. Among these novel putative export substrates, Spc72, a component of the yeast SPB, was the most interesting. Using a combination of in vitro binding assays and in vivo experiments, we showed that Spc72 fulfills the criteria for being an export substrate for Xpo1. First, binding of Xpo1 to Spc72 fragments is Gsp1-GTP dependent, and the addition of excess NES peptide competes with it. Secondly, we identified a leucine-rich amino acid sequence at position 418 to 429 in Spc72 that conforms to the NES consensus and that when mutated no longer confers binding to Xpo1. When fused to a GFP reporter or analyzed in the context of the N-terminal and C-terminal halves of Spc72, this sequence mediates nuclear export of the respective GFP fusion proteins in living yeast cells. Since Spc72 in concert with the γ-tubulin complex is required to nucleate cytoplasmic MTs at the SPB, we expected that the lack of nuclear export of NES-mutated Spc72 would result in a shortage of the protein in the cytoplasm and hence a deficiency in astral MT nucleation. Using fluorescence intensity quantification of SPBs, we found that Spc72*-GFP signals were reduced to 50% of levels observed for WT Spc72-GFP. We also observed a reduction of cytoplasmic MTs in a strain containing NES-mutated Spc72; this was also true for strains carrying mutations in *XPO1*. Taken together, these data are consistent with the notion that a functional interaction between Spc72 and Xpo1 might be required for proper spindle assembly in yeast, and they provide a first hint that nuclear export processes might be involved.

We were quite surprised to find that Xpo1 itself localizes to SPBs although the majority of the protein is found at other nuclear locations such as the NPC and the nuclear interior. In principle, this binding could be mediated by an NES-containing protein such as Spc72. However, Spc72 localizes to the cytoplasmic side of the SPB and is not required for this binding event since Xpo1 is still found at the SPB in an Spc72 deletion mutant. This suggests that Xpo1 has one or more other binding partners at the SPB, one of which could be the inner plaque protein Spc110. We found by two-hybrid analysis that it interacts with Xpo1, a fact that had not been previously analyzed. The SPB binding of Xpo1 can be reduced by overexpressing the Ran-mutant Gsp1-T26N, which lowers the Gsp1-GTP concentration in the nucleus. Although preliminary, this in vivo data might indicate that Xpo1 binding to the SPB is Ran dependent and probably mediated by an NES-containing protein other than Spc72.

What could be the function of the binding of Xpo1 to SPBs? An answer could come from what has been observed for Crm1, the Xpo1 orthologue in metazoans. Crm1 has been localized to centrosomes (22), along with Ran-GTP (37) and the NES-containing RanBP1 (15), an effector of the Ran-GTPase cycle. More recently, nucleophosmin, a multifunctional nuclear protein, has been shown to be recruited to centrosomes and Crm1 via its NES sequence (71). Treatment of cells with leptomycin B, an inhibitor of NES-Crm1 interactions, results in loss of nucleophosmin from centrosomes (61, 71). In addition, inactivating the NES of nucleophosmin by mutation had the same effect (71). Integrating all their findings in one model, these authors proposed that formation of a trimeric complex between Crm1, Ran-GTP, and an NES-containing protein such as, for example, nucleophosmin, could prevent unscheduled duplication of the centrosome during the cell cycle (8). In another study, the nuclear export of certain centrosomal proteins was shown to be inhibited by leptomycin B, but no additional data with respect to Crm1 binding or NES identification were provided (37).

Although the yeast SPB is the functional equivalent of the metazoan centrosome, it is not clear whether duplication is an analogous process in both systems (2). In addition, since budding yeast lacks nuclear envelope breakdown, mitotic spindle assembly must involve certain features unique to yeast. Although intriguing with respect to the data obtained in meta-

zoans, our findings concerning Xpo1 localization at the SPB can provide only a first hint with respect to a possible function of Xpo1 at this location. Therefore, alternative models of why and how components of the spindle apparatus and Xpo1 interact in yeast must be considered at this point.

Based on our data for Spc72, we favor the idea that Xpo1/Spc72 interaction could reflect the necessity to keep Spc72 out of the nucleus. It has been shown that fusions between the N terminus of Spc110 and the C terminus of Spc72 are functional in nucleating MTs at the cytoplasmic side of the SPB, whereas expression of the N terminus of Spc72 fused to a C-terminal fragment of Spc110 results in cell death (39). Using Xpo1 as an export receptor, the cell might restrict Spc72 to the cytoplasm, where it binds via its N terminus to the γ-tubulin complex. A sufficient amount of this complex, hence, would be anchored in the cytoplasm, initiating MT nucleation at this side of the SPB. This could explain how sorting of the Tub4 complex is achieved between the nucleus and the cytoplasm, despite the fact that cytoplasmically assembled Tub4 complexes carry an NLS sequence on Spc98, which would otherwise be used to direct all Tub4 complex into the nucleus. However, since our two-hybrid analysis did not reveal an interaction of Xpo1 and components of the Tub4 complex, the situation might be more complicated than anticipated in this model. Definitely more work is needed to characterize the regulatory mechanisms, including nuclear transport reactions that underlie spindle biogenesis in budding yeast.

ACKNOWLEDGMENTS

We thank the following people for generously providing plasmids and strains: Elizabeth Craig, Michael Knop, Peter Philippsen, Pascal Preker, Elmar Schiebel, Aaron F. Straight, and Karsten Weis. We also thank Anje Sporbert for expert advice on fluorescence intensity quantification.

This work was supported by grants of the Deutsche Forschungsgemeinschaft to G.S. and K.S.

REFERENCES

1. **Abramoff, M. D., P. J. Magelhaes, and S. J. Ram.** 2004. Image Processing with Image. J. Biophotonics Int. **11:**36–42.
2. **Adams, I. R., and J. V. Kilmartin.** 2000. Spindle pole body duplication: a model for centrosome duplication? Trends Cell Biol. **10:**329–335.
3. **Amon, A.** 2002. Synchronization procedures. Methods Enzymol. **351:**457–467.
4. **Arnaoutov, A., Y. Azuma, K. Ribbeck, J. Joseph, Y. Boyarchuk, T. Karpova, J. McNally, and M. Dasso.** 2005. Crm1 is a mitotic effector of Ran-GTP in somatic cells. Nat. Cell Biol. **7:**626–632.
5. **Bischoff, F. R., and H. Ponstingl.** 1995. Catalysis of guanine nucleotide exchange of Ran by RCC1 and stimulation of hydrolysis of Ran-bound GTP by Ran-GAP1. Methods Enzymol. **257:**135–144.
6. **Bornens, M.** 2002. Centrosome composition and microtubule anchoring mechanisms. Curr. Opin. Cell Biol. **14:**25–34.
7. **Brown, A. (ed.).** 1998. Yeast gene analysis, vol. 26. Academic Press, New York, NY.
8. **Budhu, A. S., and X. W. Wang.** 2005. Loading and unloading: orchestrating centrosome duplication and spindle assembly by Ran/Crm1. Cell Cycle **4:**1510–1514.
9. **Byers, B., and L. Goetsch.** 1975. Behavior of spindles and spindle plaques in the cell cycle and conjugation of *Saccharomyces cerevisiae*. J. Bacteriol. **124:**511–523.
10. **Carazo-Salas, R. E., O. J. Gruss, I. W. Mattaj, and E. Karsenti.** 2001. Ran-GTP coordinates regulation of microtubule nucleation and dynamics during mitotic-spindle assembly. Nat. Cell Biol. **3:**228–234.
11. **Ciciarello, M., and P. Lavia.** 2005. New CRIME plots. Ran and transport factors regulate mitosis. EMBO Rep. **6:**714–716.
12. **Dasso, M.** 2002. The Ran GTPase: theme and variations. Curr. Biol. **12:**R502–R508.
13. **Dasso, M.** 2001. Running on Ran: nuclear transport and the mitotic spindle. Cell **104:**321–324.
14. **Dasso, M., T. Seki, Y. Azuma, T. Ohba, and T. Nishimoto.** 1994. A mutant form of the Ran/TC4 protein disrupts nuclear function in *Xenopus laevis* egg extracts by inhibiting the RCC1 protein, a regulator of chromosome condensation. EMBO J. **13:**5732–5744.
15. **Di Fiore, B., M. Ciciarello, R. Mangiacasale, A. Palena, A. M. Tassin, E. Cundari, and P. Lavia.** 2003. Mammalian RanBP1 regulates centrosome cohesion during mitosis. J. Cell Sci. **116:**3399–3411.
16. **Elliott, S., M. Knop, G. Schlenstedt, and E. Schiebel.** 1999. Spc29p is a component of the Spc110p subcomplex and is essential for spindle pole body duplication. Proc. Natl. Acad. Sci. USA **96:**6205–6210.
17. **Englmeier, L., M. Fornerod, F. R. Bischoff, C. Petosa, I. W. Mattaj, and U. Kutay.** 2001. RanBP3 influences interactions between CRM1 and its nuclear protein export substrates. EMBO Rep. **2:**926–932.
18. **Fahrenkrog, B., and U. Aebi.** 2003. The nuclear pore complex: nucleocytoplasmic transport and beyond. Nat. Rev. Mol. Cell. Biol. **4:**757–766.
19. **Ferrigno, P., F. Posas, D. Koepp, H. Saito, and P. A. Silver.** 1998. Regulated nucleo/cytoplasmic exchange of HOG1 MAPK requires the importin beta homologs NMD5 and XPO1. EMBO J. **17:**5606–5614.
20. **Fischer, U., V. W. Pollard, R. Luhrmann, M. Teufel, M. W. Michael, G. Dreyfuss, and M. H. Malim.** 1999. Rev-mediated nuclear export of RNA is dominant over nuclear retention and is coupled to the Ran-GTPase cycle. Nucleic Acids Res. **27:**4128–4134.
21. **Fleig, U., S. S. Salus, I. Karig, and S. Sazer.** 2000. The fission yeast ran GTPase is required for microtubule integrity. J. Cell Biol. **151:**1101–1111.
22. **Forgues, M., M. J. Difilippantonio, S. P. Linke, T. Ried, K. Nagashima, J. Feden, K. Valerie, K. Fukasawa, and X. W. Wang.** 2003. Involvement of Crm1 in hepatitis B virus X protein-induced aberrant centriole replication and abnormal mitotic spindles. Mol. Cell. Biol. **23:**5282–5292.
23. **Fornerod, M., M. Ohno, M. Yoshida, and I. W. Mattaj.** 1997. CRM1 is an export receptor for leucine-rich nuclear export signals. Cell **90:**1051–1060.
24. **Fornerod, M., J. van Deursen, S. van Baal, A. Reynolds, D. Davis, K. G. Murti, J. Fransen, and G. Grosveld.** 1997. The human homologue of yeast CRM1 is in a dynamic subcomplex with CAN/Nup214 and a novel nuclear pore component Nup88. EMBO J. **16:**807–816.
25. **Freedman, D. A., and A. J. Levine.** 1998. Nuclear export is required for degradation of endogenous p53 by MDM2 and human papillomavirus E6. Mol. Cell. Biol. **18:**7288–7293.
26. **Fried, H., and U. Kutay.** 2003. Nucleocytoplasmic transport: taking an inventory. Cell Mol. Life Sci. **60:**1659–1688.
27. **Fukuda, M., S. Asano, T. Nakamura, M. Adachi, M. Yoshida, M. Yanagida, and E. Nishida.** 1997. CRM1 is responsible for intracellular transport mediated by the nuclear export signal. Nature **390:**308–311.
28. **Goodman, B., and Y. Zheng.** 2006. Mitotic spindle morphogenesis: Ran on the microtubule cytoskeleton and beyond. Biochem. Soc. Trans. **34:**716–721.
29. **Gruneberg, U., K. Campbell, C. Simpson, J. Grindlay, and E. Schiebel.** 2000. Nud1p links astral microtubule organization and the control of exit from mitosis. EMBO J. **19:**6475–6488.
30. **Henderson, B. R., and A. Eleftheriou.** 2000. A comparison of the activity, sequence specificity, and CRM1-dependence of different nuclear export signals. Exp. Cell Res. **256:**213–224.
31. **Hoepfner, D., A. Brachat, and P. Philippsen.** 2000. Time-lapse video microscopy analysis reveals astral microtubule detachment in the yeast spindle pole mutant cnm67. Mol. Biol. Cell **11:**1197–1211.
32. **Holtzman, D. A., S. Yang, and D. G. Drubin.** 1993. Synthetic-lethal interactions identify two novel genes, SLA1 and SLA2, that control membrane cytoskeleton assembly in *Saccharomyces cerevisiae*. J. Cell Biol. **122:**635–644.
33. **Ito, T., T. Chiba, R. Ozawa, M. Yoshida, M. Hattori, and Y. Sakaki.** 2001. A comprehensive two-hybrid analysis to explore the yeast protein interactome. Proc. Natl. Acad. Sci. USA **98:**4569–4574.
34. **James, P., J. Halladay, and E. A. Craig.** 1996. Genomic libraries and a host strain designed for highly efficient two-hybrid selection in yeast. Genetics **144:**1425–1436.
35. **Jaspersen, S. L., and M. Winey.** 2004. The budding yeast spindle pole body: structure, duplication, and function. Annu. Rev. Cell Dev. Biol. **20:**1–28.
36. **Jensen, T. H., M. Neville, J. C. Rain, T. McCarthy, P. Legrain, and M. Rosbash.** 2000. Identification of novel *Saccharomyces cerevisiae* proteins with nuclear export activity: cell cycle-regulated transcription factor Ace2p shows cell cycle-independent nucleocytoplasmic shuttling. Mol. Cell. Biol. **20:**8047–8058.
37. **Keryer, G., B. Di Fiore, C. Celati, K. F. Lechtreck, M. Mogensen, A. Delouvee, P. Lavia, M. Bornens, and A. M. Tassin.** 2003. Part of Ran is associated with AKAP450 at the centrosome: involvement in microtubule-organizing activity. Mol. Biol. Cell **14:**4260–4271.
38. **Kirkpatrick, D., and F. Solomon.** 1994. Overexpression of yeast homologs of the mammalian checkpoint gene RCC1 suppresses the class of alpha-tubulin mutations that arrest with excess microtubules. Genetics **137:**381–392.
39. **Knop, M., and E. Schiebel.** 1998. Receptors determine the cellular localization of a gamma-tubulin complex and thereby the site of microtubule formation. EMBO J. **17:**3952–3967.
40. **Kunzler, M., T. Gerstberger, F. Stutz, F. R. Bischoff, and E. Hurt.** 2000. Yeast Ran-binding protein 1 (Yrb1) shuttles between the nucleus and cyto-

plasm and is exported from the nucleus via a CRM1 (XPO1)-dependent pathway. Mol. Cell. Biol. **20:**4295–4308.
41. **Kutay, U., and S. Guttinger.** 2005. Leucine-rich nuclear-export signals: born to be weak. Trends Cell Biol. **15:**121–124.
42. **Lindsay, M. E., J. M. Holaska, K. Welch, B. M. Paschal, and I. G. Macara.** 2001. Ran-binding protein 3 is a cofactor for Crm1-mediated nuclear protein export. J. Cell Biol. **153:**1391–1402.
43. **Longtine, M. S., A. McKenzie, 3rd, D. J. Demarini, N. G. Shah, A. Wach, A. Brachat, P. Philippsen, and J. R. Pringle.** 1998. Additional modules for versatile and economical PCR-based gene deletion and modification in *Saccharomyces cerevisiae*. Yeast **14:**953–961.
44. **Maurer, P., M. Redd, J. Solsbacher, F. R. Bischoff, M. Greiner, A. V. Podtelejnikov, M. Mann, K. Stade, K. Weis, and G. Schlenstedt.** 2001. The nuclear export receptor Xpo1p forms distinct complexes with NES transport substrates and the yeast Ran binding protein 1 (Yrb1p). Mol. Biol. Cell **12:**539–549.
45. **Mosammaparast, N., and L. F. Pemberton.** 2004. Karyopherins: from nuclear-transport mediators to nuclear-function regulators. Trends Cell Biol. **14:**547–556.
46. **Murphy, M. W., B. L. Olson, and P. G. Siliciano.** 2004. The yeast splicing factor Prp40p contains functional leucine-rich nuclear export signals that are essential for splicing. Genetics **166:**53–65.
47. **Nachury, M. V., T. J. Maresca, W. C. Salmon, C. M. Waterman-Storer, R. Heald, and K. Weis.** 2001. Importin beta is a mitotic target of the small GTPase Ran in spindle assembly. Cell **104:**95–106.
48. **Neville, M., F. Stutz, L. Lee, L. I. Davis, and M. Rosbash.** 1997. The importin-beta family member Crm1p bridges the interaction between Rev. and the nuclear pore complex during nuclear export. Curr. Biol. **7:**767–775.
49. **Noguchi, E., N. Hayashi, N. Nakashima, and T. Nishimoto.** 1997. Yrb2p, a Nup2p-related yeast protein, has a functional overlap with Rna1p, a yeast Ran-GTPase-activating protein. Mol. Cell. Biol. **17:**2235–2246.
50. **Ossareh-Nazari, B., F. Bachelerie, and C. Dargemont.** 1997. Evidence for a role of CRM1 in signal-mediated nuclear protein export. Science **278:**141–144.
51. **Ouspenski, I. I.** 1998. A RanBP1 mutation which does not visibly affect nuclear import may reveal additional functions of the Ran GTPase system. Exp. Cell Res. **244:**171–183.
52. **Pemberton, L. F., and B. M. Paschal.** 2005. Mechanisms of receptor-mediated nuclear import and nuclear export. Traffic **6:**187–198.
53. **Pereira, G., M. Knop, and E. Schiebel.** 1998. Spc98p directs the yeast gamma-tubulin complex into the nucleus and is subject to cell cycle-dependent phosphorylation on the nuclear side of the spindle pole body. Mol. Biol. Cell **9:**775–793.
54. **Rodriguez, M. S., C. Dargemont, and F. Stutz.** 2004. Nuclear export of RNA. Biol. Cell **96:**639–655.
55. **Ryan, K. J., J. M. McCaffery, and S. R. Wente.** 2003. The Ran GTPase cycle is required for yeast nuclear pore complex assembly. J. Cell Biol. **160:**1041–1053.
56. **Schiebel, E.** 2000. Gamma-tubulin complexes: binding to the centrosome, regulation and microtubule nucleation. Curr. Opin. Cell Biol. **12:**113–118.
57. **Schlenstedt, G., C. Saavedra, J. D. Loeb, C. N. Cole, and P. A. Silver.** 1995. The GTP-bound form of the yeast Ran/TC4 homologue blocks nuclear protein import and appearance of poly(A)+ RNA in the cytoplasm. Proc. Natl. Acad. Sci. USA **92:**225–229.
58. **Segal, M., and K. Bloom.** 2001. Control of spindle polarity and orientation in *Saccharomyces cerevisiae*. Trends Cell Biol. **11:**160–166.
59. **Seiser, R. M., A. E. Sundberg, B. J. Wollam, P. Zobel-Thropp, K. Baldwin, M. D. Spector, and D. E. Lycan.** 2006. Ltv1 is required for efficient nuclear export of the ribosomal small subunit in *Saccharomyces cerevisiae*. Genetics **174:**679–691.
60. **Sherman, F.** 1991. Getting started with yeast, p. 3–20. *In* C. Guthrie and G. Fink (ed.), Guide to yeast genetics and molecular biology. Methods in enzymology, vol. 194. Academic Press, New York, NY.
61. **Shinmura, K., P. Tarapore, Y. Tokuyama, K. R. George, and K. Fukasawa.** 2005. Characterization of centrosomal association of nucleophosmin/B23 linked to Crm1 activity. FEBS Lett. **579:**6621–6634.
62. **Shulga, N., P. James, E. A. Craig, and D. S. Goldfarb.** 1999. A nuclear export signal prevents *Saccharomyces cerevisiae* Hsp70 Ssb1p from stimulating nuclear localization signal-directed nuclear transport. J. Biol. Chem. **274:**16501–16507.
63. **Soues, S., and I. R. Adams.** 1998. SPC72: a spindle pole component required for spindle orientation in the yeast *Saccharomyces cerevisiae*. J. Cell Sci. **111:**2809–2818.
64. **Stade, K., C. S. Ford, C. Guthrie, and K. Weis.** 1997. Exportin 1 (Crm1p) is an essential nuclear export factor. Cell **90:**1041–1050.
65. **Stade, K., F. Vogel, I. Schwienhorst, B. Meusser, C. Volkwein, B. Nentwig, R. J. Dohmen, and T. Sommer.** 2002. A lack of SUMO conjugation affects cNLS-dependent nuclear protein import in yeast. J. Biol. Chem. **277:**49554–49561.
66. **Stommel, J. M., N. D. Marchenko, G. S. Jimenez, U. M. Moll, T. J. Hope, and G. M. Wahl.** 1999. A leucine-rich nuclear export signal in the p53 tetramerization domain: regulation of subcellular localization and p53 activity by NES masking. EMBO J. **18:**1660–1672.
67. **Straight, A. F., W. F. Marshall, J. W. Sedat, and A. W. Murray.** 1997. Mitosis in living budding yeast: anaphase A but no metaphase plate. Science **277:**574–578.
68. **Taura, T., H. Krebber, and P. A. Silver.** 1998. A member of the Ran-binding protein family, Yrb2p, is involved in nuclear protein export. Proc. Natl. Acad. Sci. USA **95:**7427–7432.
69. **Tran, E. J., and S. R. Wente.** 2006. Dynamic nuclear pore complexes: life on the edge. Cell **125:**1041–1053.
70. **Usui, T., H. Maekawa, G. Pereira, and E. Schiebel.** 2003. The XMAP215 homologue Stu2 at yeast spindle pole bodies regulates microtubule dynamics and anchorage. EMBO J. **22:**4779–4793.
71. **Wang, W., A. Budhu, M. Forgues, and X. W. Wang.** 2005. Temporal and spatial control of nucleophosmin by the Ran-Crm1 complex in centrosome duplication. Nat. Cell Biol. **7:**823–830.
72. **Wen, W., J. L. Meinkoth, R. Y. Tsien, and S. S. Taylor.** 1995. Identification of a signal for rapid export of proteins from the nucleus. Cell **82:**463–473.
73. **Wiese, C., A. Wilde, M. S. Moore, S. A. Adam, A. Merdes, and Y. Zheng.** 2001. Role of importin-beta in coupling Ran to downstream targets in microtubule assembly. Science **291:**653–656.
74. **Wilde, A., S. B. Lizarraga, L. Zhang, C. Wiese, N. R. Gliksman, C. E. Walczak, and Y. Zheng.** 2001. Ran stimulates spindle assembly by altering microtubule dynamics and the balance of motor activities. Nat. Cell Biol. **3:**221–227.
75. **Winey, M., and E. T. O'Toole.** 2001. The spindle cycle in budding yeast. Nat. Cell Biol. **3:**E23–E27.
76. **Yan, C., L. H. Lee, and L. I. Davis.** 1998. Crm1p mediates regulated nuclear export of a yeast AP-1-like transcription factor. EMBO J. **17:**7416–7429.
77. **Yow, G. Y., T. Uo, T. Yoshimura, and N. Esaki.** 2004. D-Amino acid N-acetyltransferase of *Saccharomyces cerevisiae*: a close homologue of histone acetyltransferase Hpa2p acting exclusively on free D-amino acids. Arch. Microbiol. **182:**396–403.